

دهمین سمینار ملی مهندسی سطح  
۲۹ و ۳۰ اردیبهشت ماه ۸۸ - اصفهان

## Hysteresis Curves Analysis of Cyclic Indentation Tests

**A. Nayebi**

*Mechanical Engineering Department, Shiraz University*

Cyclic Vickers indentation test was modeled by finite element method. The indented material behavior was considered as nonlinear kinematic hardening. five different combinations of material model parameters were used for modeling. Maximum displacement was fixed and the variation of the maximum load and residual displacement were obtained. Their variations were found to be linear and can be used to characterize the nonlinear behavior of materials.

**Keywords :** Hysteresis, Indentation, Cyclic loading, Nonlinear kinematic hardening.

## 1. Introduction

Instrumented indentation test permits to determine many mechanical properties of materials. [1]. Montmitonnet *et al.* [2] showed that the unloading of the indentation test is not a purely elastic but plastic flow can occur because of the Bauschinger's effect. Huber and Tsakmakis [3] demonstrated that a similarity exists between a spherical indentation test and a tensile test. Because of the kinematic hardening effect the hysteresis loop can be observed in stress – strain curves of the tensile test and for the cyclic instrumented indentation test. This effect was shown experimentally [4, 5]. However, the majority of the instrumented indentation test were carried out with the isotropic strain hardening hypothesis and the unloading of the simulation was considered as elastic unloading [6]. In order to obtain the hysteresis loops in this research, which were observed experimentally, the material behavior was considered as nonlinear kinematic hardening. The Vickers instrumented indentation test was modeled by the finite element method. Maximum indenter displacement was considered constant and the variation of the maximum indenter displacement was calculated. Effects of the nonlinear kinematic hardening model parameters were studied.

## 2. Nonlinear Kinematic Hardening Model

Nonlinear kinematic hardening is introduced, choosing the form of the differential equations governing the kinematic variables. In this study the concept of the yield surface is used, which obeys the Von Mises yield criteria:

$$f = J_2(\boldsymbol{\sigma} - \mathbf{X}) - \sigma_y = \left[ \frac{3}{2} (\boldsymbol{\sigma}' - \mathbf{X}') : (\boldsymbol{\sigma}' - \mathbf{X}') \right]^{\frac{1}{2}} - \sigma_y = 0 \quad (1)$$

$\mathbf{X}$  is the back stress which defines position of the yield surface and  $\sigma_y$  is the size of the surface. The plastic flow follows the normality rule:

$$d\boldsymbol{\varepsilon}^p = d\lambda \frac{\partial f}{\partial \boldsymbol{\sigma}} = \frac{3}{2} d\lambda \frac{\boldsymbol{\sigma}' - \mathbf{x}'}{(\boldsymbol{\sigma}' - \mathbf{x}')_{eq}} \quad (2)$$

The plastic multiplier  $d\lambda$  is derived from the consistency condition,  $f = df = 0$ , if plastic flow occurs. Different kinematic hardening models are available for the plastic analysis of structures. In this paper, the Non linear kinematic hardening model [7] was used for the non linear strain hardening materials. If the plastic strain ( $\boldsymbol{\varepsilon}_{ij}^p$ ) and the back stress tensor ( $\mathbf{X}_{ij}$ ) are assumed as the internal variables, the evolution equations are:

(a) Flow rule:

$$d\boldsymbol{\varepsilon}_{ij}^p = d\lambda n_{ij} \quad (3)$$

where  $n_{ij} = \frac{\partial f}{\partial \sigma_{ij}} = \frac{3}{2} \frac{\sigma'_{ij} - X'_{ij}}{\|\boldsymbol{\sigma}'_{ij} - \mathbf{X}'_{ij}\|}$  is the outward normal to the yield surface and  $d\lambda$  is the

increment of the plastic multiplier calculated from the consistency condition:

$$df = \frac{\partial f}{\partial \sigma_{ij}} d\sigma_{ij} + \frac{\partial f}{\partial X_{ij}} dX_{ij} \quad (4)$$

(b) Non linear kinematic hardening model:

$$dX_{ij} = 2/3 C d\boldsymbol{\varepsilon}_{ij}^p + \gamma X_{ij} dp \quad (5)$$

where  $C$  and  $\gamma$  are the materials positive constant values and

$$dp = \left( \frac{2}{3} d\varepsilon_{ij}^p d\varepsilon_{ij}^p \right)^{\frac{1}{2}} \quad (6)$$

### 3. Finite Element Simulation

Simulation of the Vickers indentation process was performed using the Cast3M [8] finite element (FE) software. In figure 1, the geometry of the Vickers indentation test is shown schematically. A Cartesian formulation was employed using a xyz coordinate system with horizontal coordinate,  $x$ , and vertical coordinate,  $z$ . It is assumed that a deformable Vickers indenter with high Young modulus penetrating a homogenous, isotropic, rate independent, semi infinite body. Due to the eight fold symmetry of deformation, only  $1/8^{\text{th}}$  of the body needs to be modeled as indicated in figure 1. A key issue for the accuracy and efficiency of the FEM computations was the development of an appropriate mesh which approximated the semi-infinite body. The mesh proposed by Giannakopoulos *et al* [9] was used. It is shown in figure 2(a) which is bounded by 5 surfaces. Roller boundary conditions were applied at the bottom surface by enforcing no displacements in the  $z$  direction and free movement in the  $x$  and  $y$  directions. Symmetry boundary conditions were applied along the centerline, and a free surface was modeled at the outside of the specimen and on the top surface outside the region of contact. The nodes of the surfaces  $S_r$  and  $S_l$  can deform only in their own planes. The mesh independency of the results was tested. The mesh shown in figure 3 was constructed for the Vickers analysis with the following characteristics: 7620 eight-nodded isoparametric block elements and 8741 nodes. In the elastoplastic analysis the contact area covered at least 10 elements.

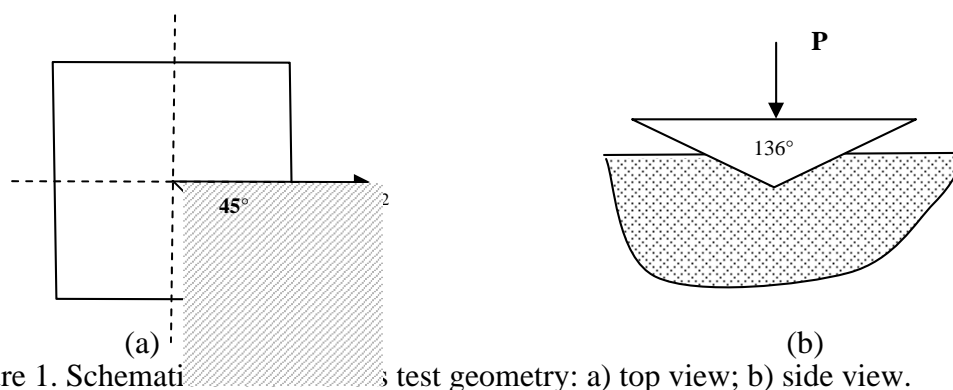


Figure 1. Schematic of Vickers test geometry: a) top view; b) side view.

The resulting mechanical problem concerns a homogeneous and isotropic half-space indented in the normal direction to the surface by a Vickers indenter as shown in figure 1. It is assumed that the resulting deformation takes place under quasi-static and isothermal conditions. Furthermore, only frictionless contact between the indenter and the half-space is considered. The latter assumption is acceptable in the present situation as mainly global properties are at stake and frictional effects on such variables are known; cf. e.g. Carlsson *et al.* [10]. The calculations were performed under finite strain assumptions for both loading and unloading conditions.

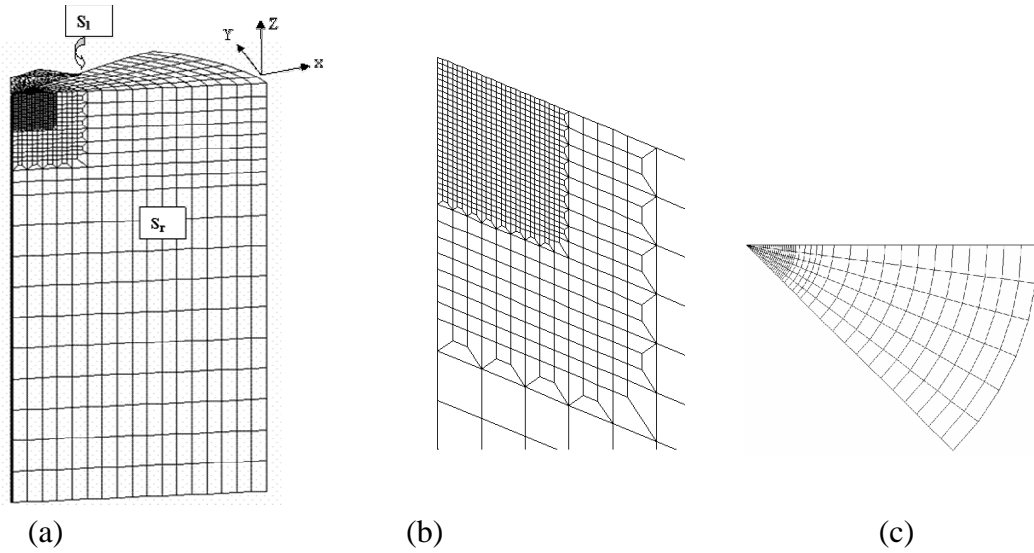


Figure 2. Finite element mesh used in elastoplastic analysis of the Vickers indentation: a) general view; b) detail of the mesh at the contact region; c) top view.

**4. Results and Discussions**

Simulations were carried out with nonlinear kinematic hardening model of Armstrong – Frederick (equation (5)). The figure 3 shows the variation of the applied force as a function of the indenter displacement with hysteresis loops for a ductile steel which the mechanical properties are:  $E=200$  GPa,  $\nu=0,3$ ,  $\sigma_y =300$  MPa,  $C= 500$  MPa and  $\gamma=60$ . As it was shown in the figure 1, the hysteresis loops were obtained during loading and unloading despite of the isotropic strain theory simulation results. If the maximum indenter displacement is limited to  $8 \mu\text{m}$ , the hysteresis loops approach together and they are stabilized. Thus it seems possible to be able to extract the parameters of the nonlinear kinematic hardening model by a cyclic test of indentation. In order to obtain the hysteresis loops  $C$  parameter was changed between 250 and 500 MPa and  $\gamma$  between 5 and 50. Residual displacement for each cycle was normalized by the maximum displacement of first cycle. The maximum effort of each cycle was divided by the maximum effort of first cycle. Table 1 shows the parameters used for modeling of the cyclic tests.

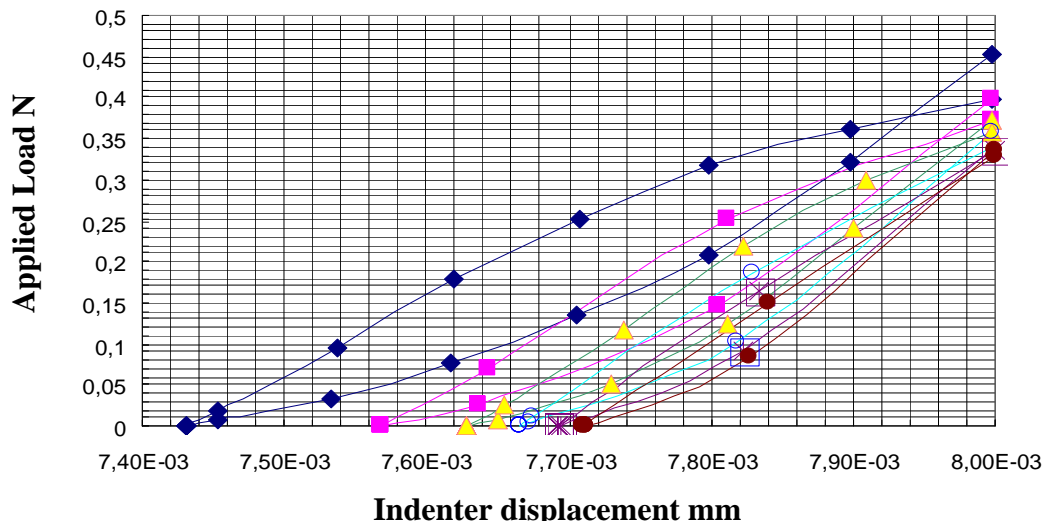


Figure 3. Hysteresis loops of the indenter displacement – applied load curve.

Table 1. Parameters of the Armstrong – Freidrick model used for FEM simulations.

Case	E GPa	$\nu$	$\sigma_y$ MPa	C MPa	$\gamma$
A	210	0,3	300	250	50
B	210	0,3	300	500	10
C	210	0,3	300	500	50
D	210	0,3	300	500	5
E	210	0,3	600	500	50

Figures 4 to 8 show the curves of  $F_{\max}^i/F_{\max}^1$  as a function of  $\delta_r/\delta_{\max}$ . As it can be seen, the curve is linear for all the combinations of the parameters. For two cases of C and E, with increasing the yield stress the normalized applied load decreases. Parameter C has the same influence on the indentation load. But the influence of the  $\gamma$  parameter is less important.

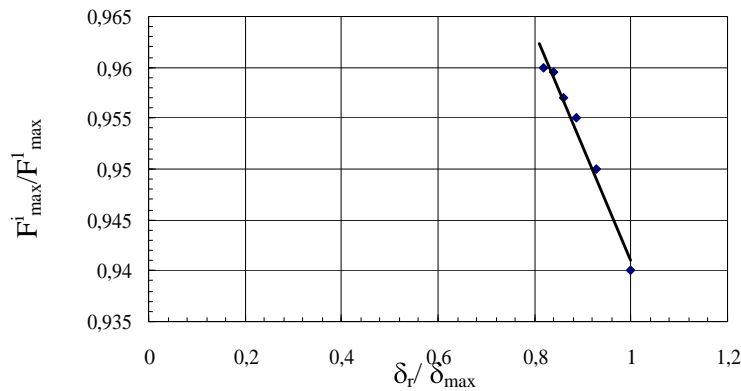


Figure 4. Variation of  $F_{\max}^i/F_{\max}^1$  as a function of  $\delta_r/\delta_{\max}$  for the case A in the Table 1.

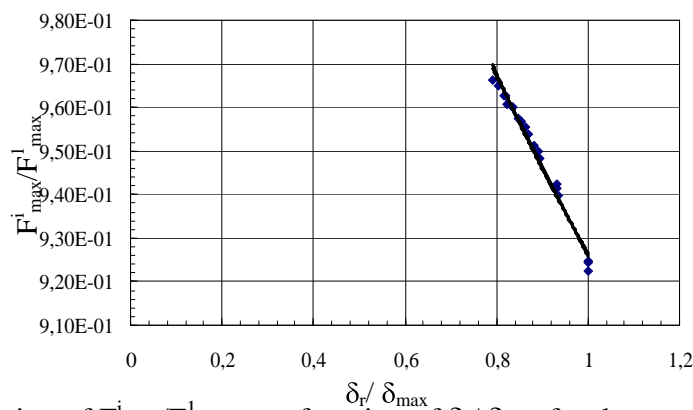


Figure 5. Variation of  $F_{\max}^i/F_{\max}^1$  as a function of  $\delta_r/\delta_{\max}$  for the case B in the Table 1.

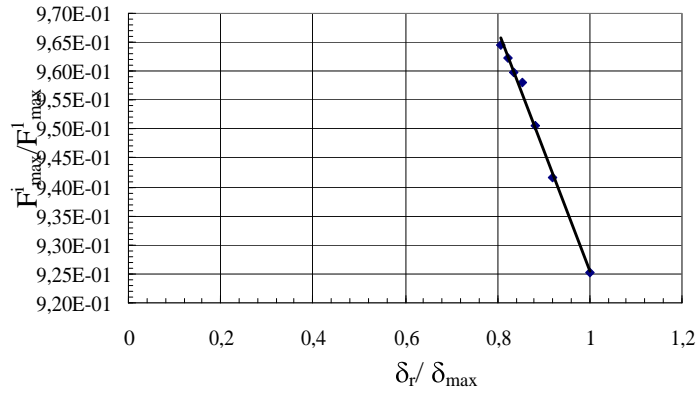


Figure 6. Variation of  $F_{max}^i / F_{max}^1$  as a function of  $\delta_r / \delta_{max}$  for the case C in the Table 1.

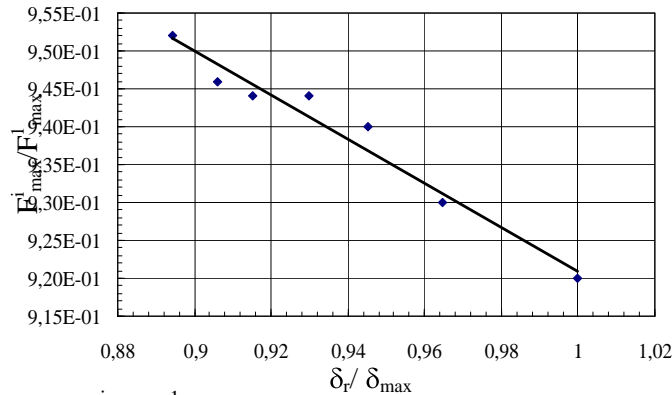


Figure 7. Variation of  $F_{max}^i / F_{max}^1$  as a function of  $\delta_r / \delta_{max}$  for the case D in the Table 1.

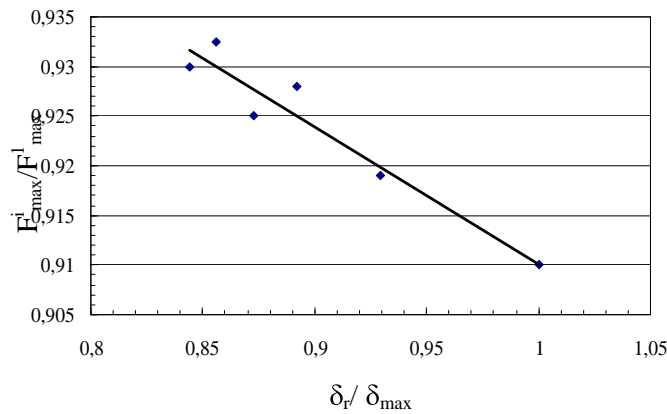


Figure 8. Variation of  $F_{max}^i / F_{max}^1$  as a function of  $\delta_r / \delta_{max}$  for the case E in the Table 1.

### 5. Conclusion

Cyclic Vickers indentation test was modeled by finite element method. A new idea was presented in order to characterize nonlinear kinematic hardening properties of metals by a cyclic indentation test. By carrying out the cyclic test of Vickers, maximum displacement is fixed. The variations of the maximum effort and residual displacement for different combination of nonlinear kinematic hardening model parameters were

obtained. This variation is linear and can be used in the nonlinear characterization of the behaviors.

### References

- [1] A. Nayebi, R. El Abdi, O. Bartier and G. Mauvoisin, *Mechanics of Materials* Vol. 34, 2002, pp. 243-254.
- [2] P. Montmitonnet, M.L. Edlinger, E. Felder, Finite element analysis of elastoplastic indentation. Part I : homogeneous media, *J. Tribology (Trans. ASME)*, Vol. 115, 1993, pp. 10-14.
- [3] N. Huber and Ch. Tsakmakis, Experimental and theoretical investigation of the effect of kinematic hardening on spherical indentation. *Mechanics of Materials*, Vol. 27, 1998, Pages 241-248
- [4] N. Huber and Ch. Tsakmakis, Determination of constitutive properties from spherical indentation data using neural networks. Part I: the case of pure kinematic hardening in plasticity laws, *J. of the Mechanics and Physics of Solids*, Vol. 47, 1999, pp. 1569-1588
- [5] N. Huber and Ch. Tsakmakis, Determination of constitutive properties from spherical indentation data using neural networks. Part II: plasticity with nonlinear isotropic and kinematic hardening, *J. of the Mechanics and Physics of Solids*, Vol. 47, 1999, pp. 1589-1607
- [6] A. Nayebi, New Instrumented Indentation Methods to assess Mechanical Properties., هفتمین کنفرانس ملی مهندسی سطح و عملیات حرارتی, دانشگاه صنعتی اصفهان, اردیبهشت ۱۳۸۵
- [7] Armstrong, P.J. and Frederick, C.O., A Mathematical Representation of the Multi-axial Bauschinger Effect, G.E.G.B. Report RD/B/N 731, 1966.
- [8] Millard, A., Castem 2000, Guide du development. *Rapport D.E.M.T./92 300, C.E.A*, (1992).
- [9] Giannakopoulos, A.E. Larsson, P.-L. and Vestergaard, R. "Analysis of Vickers indentation." *Int. J. Solids Structures*, Vol. 31, 1994, pp. 2679-2708.
- [10] Carlsson, S. Biwa, S. Larsson, P.-L. On frictional effects at inelastic contact between spherical bodies. *Int. J. Mechanical sciences*, Vol. 42, 1999, pp. 107-128.